# Formation Control with Multiplex Information Networks

Dzung Tran, Tansel Yucelen, and Eduardo Pasiliao

*Abstract*—Current distributed control methods have a lack of information exchange infrastructure to enable spatially evolving multiagent formations. Specifically, these methods are designed based on information exchange rules represented by a network having a single layer, where they lead to multiagent formations with fixed, non-evolving spatial properties. For situations where capable agents have to control the resulting formation through these methods, they can often do so if such agents have global information exchange ability. Yet, global information exchange is not practical for cases that have large numbers of agents and low-bandwidth peer-to-peer communications. Motivated from this standpoint, the contribution of this paper is to show how information exchange rules, which are represented by a network having multiple layers (multiplex information networks), can be designed for enabling spatially evolving multiagent formations. In particular, we first consider the formation assignment problem and then the formation tracking problem, and introduce new distributed control architectures that allow capable agents to spatially alter the size and the orientation of the resulting formation without requiring global information exchange ability. In addition, tools and methods from differential potential fields are further utilized in order to generalize the proposed distribute control architecture for the formation tracking problem to allow for connectivity maintenance and collision avoidance needed in real-world applications. Stability of the proposed architectures is theoretically analyzed and their efficacy are illustrated on numerical examples and on multiagent formation experiments.

## I. INTRODUCTION

As advances in VLSI and MEMS technologies have boosted the development of integrated systems that combine mobility, computing, communication, and sensing on a single platform, future civilian and military operations will have the capability to exploit large numbers of interconnected agents such as low-cost and small-in-size autonomous vehicles and microsensors. Such large-scale multiagent systems will support operations ranging from environment monitoring and military surveillance, to guidance, navigation, and control of autonomous underwater, ground, aerial, and space vehicles. For performing operations with dramatically increasing levels of complexity, multiagent systems require advanced distributed information exchange rules in order to make these systems evolve spatially for adapting dynamic environments and effectively responding to human interventions. Yet, current distributed control methods lack information exchange infrastructures to enable spatially evolving multiagent formations. This is due to the fact that these methods are designed based on information exchange rules for a network having a single layer (see, for

example, [1]–[3] and references therein), which leads to multiagent formations with fixed, non-evolving spatial properties. For situations where capable agents [1] have to control the resulting formation through these methods, they can often do so if such vehicles have global information exchange ability, but this is not practical for cases with large numbers of agents and low-bandwidth peer-to-peer communications.

### A. Contribution

The contribution of this paper is to introduce and show how information exchange rules, which are represented by a network having multiple layers (multiplex information networks), can be designed for enabling spatially evolving multiagent formations. In particular, after stating necessary mathematical preliminaries in Section II, we first consider the formation assignment problem (i.e., creating a desired formation for the multiagent system in hand) in Section III and then the formation tracking problem (i.e., formation control while tracking a dynamic, non-stationary target) in Section IV, and introduce new distributed control architectures that allow capable agents to spatially alter the size and the orientation of the resulting formation[2] without requiring global information exchange ability. In addition, tools and methods from differential potential fields are further utilized in Section IV in order to generalize the proposed distribute control architecture for the formation tracking problem to allow for connectivity maintenance and collision avoidance needed in real-world applications. Stability of the proposed architectures is theoretically analyzed and their efficacy are illustrated on numerical examples in Sections III and IV and on multiagent formation experiments in Section V.

### B. Related Literature

Studies on multiplex information networks have recently emerged in the physics and networks science literatures, where they consider system-theoretic characteristics of network dynamics with multiple layers subject to intralayer and interlayer information exchange [4]–[11] (there also exist studies on multiplex networks that do not consider system-theoretic characteristics; see [12] for a survey). However, these studies mainly consider cases where all layers perform simple consensus algorithms and analyze the convergence of the overall multiagent systems in the presence of not only intralayer but also interlayer information exchange, and hence, they

[1]Capable agents denote a subset (or at least one) of all agents in a given multiagent system, which have the knowledge of desired parameters used to control resulting formations.

[2]In this paper, spatial size control means to scale the original desired distances between agents through a design parameter only available to capable agents and spatial orientation control means to rotate the original multiagent formation by a rotation matrix constructed with a design parameter only available to these capable agents.

do not deal with controlling spatial properties of multiagent formations. Note that there are also recent studies on networks of networks by the authors of [13]–[15]. However, these studies deal with large-scale systems formed from smaller factor networks via graph Cartesian products; hence, they are also not related with the contribution of this paper.

Spatial multiagent formation control is considered by the authors of [16]–[19] using approaches different from multiplex information networks. In particular, the authors of [16]–[18] assume that some of the formation design parameters are known globally by all agents, and the authors of [19] assume global knowledge of the complete network at the analysis stage. However, as previously discussed, such assumptions may not be practical in the presence of large numbers of agents and low-bandwidth peer-to-peer communications. From a data security point of view, in addition, it should be noted that one may not desire a multiagent system with all agents sharing some global information about an operation of interest. Throughout this paper, we do not make such assumptions in our multiplex information networks-based spatial multiagent formation control approach. Finally, two preliminary conference versions of this paper appeared in [20], [21]. The present paper considerably expands on [20], [21] by providing detailed proofs of all the results with additional motivation, examples, and multiagent formation experiments.

## II. MATHEMATICAL PRELIMINARIES

We now introduce this paper's notation and recall basic notions from graph theory, which are followed by the general setup of consensus and formation problems for multiagent systems that are necessary to establish our main results[3].

### A. Notation and Notions from Graph Theory

Throughout this paper, $\mathbb{R}$ denotes the set of real numbers, $\mathbb{R}^n$ denotes the set of $n \times 1$ real column vectors, $\mathbb{R}^{n \times m}$ denotes the set of $n \times m$ real matrices, $\mathbb{R}_+$ (resp., $\overline{\mathbb{R}}_+$) denotes the set of positive (resp., non-negative) real numbers, $\mathbb{R}_+^{n \times n}$ (resp., $\overline{\mathbb{R}}_+^{n \times n}$) denotes the set of $n \times n$ positive-definite (resp., non-negative-definite) real matrices, $0_n$ denotes the $n \times 1$ vector of all zeros, $\mathbf{1}_n$ denotes the $n \times 1$ vector of all ones, $0_{n \times n}$ denotes the $n \times n$ zero matrix, $\mathrm{I}_n$ denotes the $n \times n$ identity matrix, and $\otimes$ denotes the Kronecker product operation. In addition, we write $(\cdot)^{\mathrm{T}}$ for transpose, $\lambda_{\min}(A)$ and $\lambda_{\max}(A)$ for the minimum and maximum eigenvalue of the Hermitian matrix A, respectively; $\lambda_i(A)$ for the $i$-th eigenvalue of A, where A is symmetric and the eigenvalues are ordered from least to greatest value, $\det(A)$ for the determinant of $A$, $\mathrm{diag}(a)$ for the diagonal matrix with the vector $a$ on its diagonal, $[x]_i$ for the entry of the vector $x$ on the $i$-th row, and $[A]_{ij}$ for the entry of the of the matrix A on the $i$-th row and $j$-th column. Furthermore, for given functions $f(t)$ and $g(t)$, $f(t) \to g(t)$ as $t \to \infty$ denotes $\lim_{t \to \infty} \big( f(t) - g(t) \big) = 0$.

In the multiagent systems literature, graphs are broadly adopted to encode interactions between networked agents. An undirected graph $\mathcal{G}$ is defined by a set $\mathcal{V}_\mathcal{G} = \{1, \ldots, n\}$ of nodes and a set $\mathcal{E}_\mathcal{G} \subset \mathcal{V}_\mathcal{G} \times \mathcal{V}_\mathcal{G}$ of edges. If the distance between two arbitrary nodes is less than $R$, then they are said

to be neighbors and the neighboring relation is denoted by $j \in \mathcal{N}_i \triangleq \{j| \ j \in \mathcal{V}_\mathcal{G}, \|x_{ij}\|_2 < R\}$, where $x_{ij} \triangleq x_i - x_j$ with $x_i$ and $x_j$ being the state (position) of nodes $i$ and $j$, respectively. In addition, if $(i, j) \in \mathcal{E}_\mathcal{G}$, then the nodes $i$ and $j$ are said to be formation neighbors [23], [24] and this relation is denoted by $j \in \mathcal{N}_i^f$, where $\mathcal{N}_i^f$ is a subset of $\mathcal{N}_i$. In general, note that $\mathcal{N}_i$ can be a time-varying set while $\mathcal{N}_i^f$ is a static set, that is, $\mathcal{N}_i^f$ remains unchanged in the presence of node movements. The degree of a node is given by the number of its formation neighbors. In particular, letting $d_i$ be the degree of node $i$, the degree matrix of a graph $\mathcal{G}$, $\mathcal{D}(\mathcal{G}) \in \mathbb{R}^{n \times n}$, is given by $\mathcal{D}(\mathcal{G}) = \mathrm{diag}(d)$, $d = [d_1, \ldots, d_n]^{\mathrm{T}}$. A path $i_0 i_1 \ldots i_L$ is a finite sequence of nodes such that $i_{k-1} \in \mathcal{N}_{i_k}^f$ with $k = 1, \ldots, L$, and a graph $\mathcal{G}$ is connected if there exists a path between any pair of distinct nodes. The adjacency matrix of a graph $\mathcal{G}$, $\mathcal{A}(\mathcal{G}) \in \mathbb{R}^{n \times n}$, is given by $[\mathcal{A}(\mathcal{G})]_{ij} = 1$ if $(i, j) \in \mathcal{E}_\mathcal{G}$ and $[\mathcal{A}(\mathcal{G})]_{ij} = 0$ otherwise. The Laplacian matrix of a graph, $\mathcal{L}(\mathcal{G}) \in \overline{\mathbb{R}}_+^{n \times n}$, is given by $\mathcal{L}(\mathcal{G}) \triangleq \mathcal{D}(\mathcal{G}) - \mathcal{A}(\mathcal{G})$, where the spectrum of the Laplacian for an undirected and connected graph $\mathcal{G}$ can be ordered as $0 = \lambda_1(\mathcal{L}(\mathcal{G})) < \lambda_2(\mathcal{L}(\mathcal{G})) \leq \cdots \leq \lambda_n(\mathcal{L}(\mathcal{G}))$ with $\mathbf{1}_n$ as the eigenvector corresponding to the zero eigenvalue $\lambda_1(\mathcal{L}(\mathcal{G}))$ and $\mathcal{L}(\mathcal{G})\mathbf{1}_n = 0_n$ and $\mathrm{e}^{\mathcal{L}(\mathcal{G})}\mathbf{1}_n = \mathbf{1}_n$ hold. Here, we assume graph $\mathcal{G}$ is undirected and connected unless noted otherwise.

### B. Consensus and Formation Dynamics

A graph $\mathcal{G}$ can model a given multiagent system with nodes and edges respectively representing agents and interagent information exchange links. Specifically, let $x_i(t) \in \mathbb{R}^m$ denote the state of node $i$, whose dynamics is described by the single integrator $\dot{x}_i(t) = u_i(t)$, $x_i(0) = x_{i0}$, $i = 1, \cdots, n$, with $u_i(t) \in \mathbb{R}^m$ being the control input of node $i$. Allowing agent $i$ to have access to the relative state information with respect to its formation neighbors, a solution to the consensus problem can be achieved, for example, by applying $u_i(t) = -\sum_{j \in \mathcal{N}_i^f} \big( x_i(t) - x_j(t) \big)$ to the above single integrator dynamics [1], [2], where the resulting dynamics can be represented by the Laplacian dynamics of the form

$$\dot{x}(t) = -\mathcal{L}(\mathcal{G}) \otimes \mathrm{I}_m \, x(t), \quad x(0) = x_0, \qquad (1)$$

with $x(t) = [x_1^{\mathrm{T}}(t), \cdots, x_n^{\mathrm{T}}(t)]^{\mathrm{T}}$ denoting aggregated state vector of multiagent system. Since the graph $\mathcal{G}$ is undirected and connected, $\lim_{t \to \infty} [x_i(t)]_j = \big( [x_1(0)]_j + \cdots [x_n(0)]_j \big)/n$ holds from (1) for $i = 1, \ldots, n$ and $j = 1, \ldots, m$. In this paper, we assume that $m = 2$ without loss of generality, which implies that the multiagent system evolves in a planar space.

On the formation problem, define $x_i(t) - \xi_i \in \mathbb{R}^2$ as the displacement of $x_i(t) \in \mathbb{R}^2$ from the desired formation position of agent $i$, $\xi_i \in \mathbb{R}^2$. Using now the transformed state $x_i(t) - \xi_i$ instead of $x_i(t)$ in (1) for $i = 1, \ldots, n$, one can write the dynamics $\dot{x}(t) = -\big( \mathcal{L}(\mathcal{G}) \otimes \mathrm{I}_2 \big) x(t) + \big( \mathcal{L}(\mathcal{G}) \otimes \mathrm{I}_2 \big) \xi$, $x(0) = x_0$, [1], [2], where $\xi = [\xi_1, \cdots, \xi_n]^{\mathrm{T}}$. Note that the above expression addressing the formation problem with $m = 2$ can equivalently be written as $\dot{x}_i(t) = -\sum_{j \in \mathcal{N}_i^f} \big( x_i(t) - x_j(t) \big) + \sum_{j \in \mathcal{N}_i^f} \big( \xi_i - \xi_j \big)$, $x_i(0) = x_{i0}$. In the rest of this paper, we consider a generalized version of this benchmark formation problem that not only allows to create a desired formation for the multiagent system in hand

---

[3]For details about graph theory and multiagent systems, see [1], [2], [22].

(i.e., formation assignment; see Section III) but also allows formation control while tracking a dynamic, non-stationary target (i.e., formation tracking problem; see Section IV). In our proposed algorithm, the original resulting formation as well as the desired position of agent $i$ represented by $\xi_i$ are oriented through the rotation matrix $R(\theta_i(t))$ and the size is controlled by the term $\gamma_i(t)$; thus, the resulting formation is now represented by $\gamma_i(t)R(\theta_i(t))\xi_i$ for $i = 1,\ldots,n$. In addition, the desired scaling design parameter $\gamma(t)$ and the desired rotation angle design parameter $\theta(t)$ are both locally spread out in the network via two separate layers, and $\gamma_i(t)$ and $\theta_i(t)$ asymptotically converge to these design parameter values. This then allows for spatial control of both the size and orientation of a given original multiagent formation. Although we consider this particular formation problem in this paper, the presented multiplex information networks-based approach can be extended to many other approaches to formation control. Finally, for the purpose of directly focusing on our main contribution stated in Section I.A, we assume in this paper that the interactions between agents are not subject to time-delays. For practical applications when interaction time-delays are not negligible and significant, one can consider the results in, for example, [25]–[30] for analytically extending the results of this paper to the time-delay case.

## III. SPATIAL CONTROL OF MULTIAGENT SYSTEMS IN FORMATION ASSIGNMENT

This section focuses on the formation assignment problem, where we introduce and analyze a multiplex information networks-based distributed control architecture for spatially controlling both size and orientation of multiagent formations (Section III.A). Then, we illustrate the result by a numerical example (Section III.B).

### A. Formation Density and Orientation Control

Consider a system of $n$ agents exchanging information among each other using their local measurements, according to an undirected and connected graph $\mathcal{G}$. Based on the benchmark formation problem outlined in Section II.B, we also consider that $\xi_i$ and $\xi_j$ are locally available to each agent, where this captures an original, desired planar (i.e., $m = 2$) formation. In addition, we consider that there is a subset of agents (or at least one agent), i.e., capable agents, that has the knowledge of the desired scaling parameter $\gamma(t)$ and the desired rotation angle $\theta(t)$. To this end, we focus on the problem of developing local information exchange rules for enabling spatial control of size and orientation of the original planar formation through parameters $\gamma(t)$ and $\theta(t)$ available only to a subset of agents (i.e., capable agents). Motivated from this standpoint, we propose the distributed controller having three layers[4]

$$\dot{x}_i(t) = -\sum_{j\in\mathcal{N}_i^f}\big(x_i(t) - x_j(t)\big)$$
$$+\sum_{j\in\mathcal{N}_i^f}\Big(\gamma_i(t)R(\theta_i(t))\xi_i - \gamma_j(t)R(\theta_j(t))\xi_j\Big)$$
$$+\dot{\gamma}_i(t)R(\theta_i(t))\xi_i + \gamma_i(t)\dot{R}(\theta_i(t))\xi_i,$$

[4]The right hand side of (2) coupled with (3) and (4) represents the local controller $u_i(t)$ for agent dynamics of the form $\dot{x}_i(t) = u_i(t)$.

$$x_i(0) = x_{i0}, \quad (2)$$

$$\dot{\gamma}_i(t) = -\sum_{j\in\mathcal{N}_i^f}\big(\gamma_i(t) - \gamma_j(t)\big) - k_i\big(\gamma_i(t) - \gamma(t)\big)$$
$$-\tau_\gamma\mathrm{sgn}\Big(\sum_{j\in\mathcal{N}_i^f}\big(\gamma_i(t) - \gamma_j(t)\big) + k_i\big(\gamma_i(t) - \gamma(t)\big)\Big),$$

$$\gamma_i(0) = \gamma_{i0}, \quad (3)$$

$$\dot{\theta}_i(t) = -\sum_{j\in\mathcal{N}_i^f}\big(\theta_i(t) - \theta_j(t)\big) - k_i\big(\theta_i(t) - \theta(t)\big)$$
$$-\tau_\theta\mathrm{sgn}\Big(\sum_{j\in\mathcal{N}_i^f}\big(\theta_i(t) - \theta_j(t)\big) + k_i\big(\theta_i(t) - \theta(t)\big)\Big),$$

$$\theta_i(0) = \theta_{i0}, \quad (4)$$

where $x_i(t) \in \mathbb{R}^2$ denotes the state of the first layer of agent $i$ that corresponds to the actual state of agent $i$, $\xi_i \in \mathbb{R}^2$ denotes the original formation shape of agent $i$, $\gamma_i(t) \in \mathbb{R}$ denotes the state of the second layer of agent $i$ that is introduced to distribute the formation scaling parameter or size factor $\gamma(t) \in \mathbb{R}$ through local information exchange, $\theta_i(t) \in \mathbb{R}$ denotes the state of the third layer of agent $i$ that is introduced to distribute the formation orientation parameter or rotation angle $\theta(t) \in \mathbb{R}$ through local information exchange, and $k_i = 1$ for capable agents (a subset or at least one of the $n$ agents in the multiagent system) and otherwise $k_i = 0$. In (2), $R(\theta_i(t))$ denotes the rotation matrix of agent $i$

$$R(\theta_i(t)) \triangleq \begin{bmatrix} \cos\theta_i(t) & -\sin\theta_i(t) \\ \sin\theta_i(t) & \cos\theta_i(t) \end{bmatrix} \in \mathbb{R}^{2\times2}. \quad (5)$$

Note that the desired formation scaling factor $\gamma(t)$ and rotation angle $\theta(t)$ are considered to be bounded and continuously differentiable, and only available to capable agents as such they have the capability to alter the size and orientation of the resulting formation (i.e., scale and rotate the formation). Similar to [31], we also assume $\dot{\gamma}(t)$ and $\dot{\theta}(t)$ are bounded such that $|\dot{\gamma}(t)| \leq \omega_\gamma$ and $|\dot{\theta}(t)| \leq \omega_\theta$, and $\tau_\gamma$ and $\tau_\theta$ are chosen such that $\tau_\gamma > \omega_\gamma$ and $\tau_\theta > \omega_\theta$.

It should be also further emphasized that the first layer represented by (2) helps in forming the desired formation while the second and third layers represented by (3) and (4) respectively allow the scaling factor $\gamma(t)$ and the rotation angle $\theta(t)$ to be spread out in the network and be updated in the first layer; hence, the formation size and orientation can be controlled. The next theorem presents our first result.

**Theorem 1.** Consider the networked multiagent system given by (2), (3), and (4), where agents exchange information using local measurements and with $\mathcal{G}$ defining an undirected and connected graph topology. Then,

$$\lim_{t\to\infty}\Big(\big(x_i(t) - x_j(t)\big) - \gamma(t)R\big(\theta(t)\big)\big(\xi_i - \xi_j\big)\Big) = 0, \quad (6)$$

holds for all $i = 1,\ldots,n$ and $j \in N_i^f$.

*Proof.* First, we prove that under the two underlying layers (3) and (4), $\gamma_i(t)$ and $\theta_i(t)$ converge to desired parameters $\gamma(t)$ and $\theta(t)$ for all $i = 1,\ldots,n$. Let us consider the state transformations given by $\tilde{\gamma}_i(t) \triangleq \gamma_i(t) - \gamma(t)$, $i = 1,\ldots,n$, and $\tilde{\theta}_i(t) \triangleq \theta_i(t) - \theta(t)$, $i = 1,\ldots,n$. Using the first state transformation with (3) yields

$$\dot{\tilde{\gamma}}_i(t) = - \sum_{j \in \mathcal{N}_i^f} \big( \tilde{\gamma}_i(t) - \tilde{\gamma}_j(t) \big) - k_i \tilde{\gamma}_i(t)$$
$$- \tau_\gamma \mathrm{sgn}\Big( \sum_{j \in \mathcal{N}_i^f} \big( \tilde{\gamma}_i(t) - \tilde{\gamma}_j(t) \big) + k_i \tilde{\gamma}_i(t) \Big) - \dot{\gamma}(t), \quad (7)$$

and using the second state transformation with (4) yields

$$\dot{\tilde{\theta}}_i(t) = - \sum_{j \in \mathcal{N}_i^f} \big( \tilde{\theta}_i(t) - \tilde{\theta}_j(t) \big) - k_i \tilde{\theta}_i(t)$$
$$- \tau_\theta \mathrm{sgn}\Big( \sum_{j \in \mathcal{N}_i^f} \big( \tilde{\theta}_i(t) - \tilde{\theta}_j(t) \big) + k_i \tilde{\theta}_i(t) \Big) - \dot{\theta}(t). \quad (8)$$

By letting $\tilde{\gamma}(t) \triangleq \big[\tilde{\gamma}_1(t), \dots, \tilde{\gamma}_n(t)\big]^{\mathrm{T}}$, $\tilde{\theta}(t) \triangleq \big[\tilde{\theta}_1(t), \dots, \tilde{\theta}_n(t)\big]^{\mathrm{T}}$, the expressions (7) and (8) can be equivalently written in a compact form as

$$\begin{aligned}\dot{\tilde{\gamma}}(t) &= -\big(\mathcal{L}(\mathcal{G}) + K\big)\tilde{\gamma}(t) \\ &\quad - \tau_\gamma \mathrm{sgn}\Big( \big(\mathcal{L}(\mathcal{G}) + K\big)\tilde{\gamma}(t) \Big) - \mathbf{1}_n \dot{\gamma}(t), \quad (9)\end{aligned}$$

$$\begin{aligned}\dot{\tilde{\theta}}(t) &= -\big(\mathcal{L}(\mathcal{G}) + K\big)\tilde{\theta}(t) \\ &\quad - \tau_\theta \mathrm{sgn}\Big( \big(\mathcal{L}(\mathcal{G}) + K\big)\tilde{\theta}(t) \Big) - \mathbf{1}_n \dot{\theta}(t), \quad (10)\end{aligned}$$

where $K \triangleq \mathrm{diag}\big([k_1, \dots, k_n]^{\mathrm{T}}\big)$. Since $\dot{\tilde{\gamma}}$ and $\dot{\tilde{\theta}}$ have the same structure, we only show the analysis for $\tilde{\gamma}(t)$ here, but the analysis for $\tilde{\theta}(t)$ is similar. Now, consider the Lyapunov function candidate $V(\tilde{\gamma}) = \frac{1}{2}\tilde{\gamma}^T(\mathcal{L}(\mathcal{G}) + K)\tilde{\gamma}$, and so its time derivative along the trajectory of (9) is given by

$$\begin{aligned}\dot{V}(\tilde{\gamma}(t)) &= \tilde{\gamma}^T(\mathcal{L}(\mathcal{G}) + K)\bigg( -(\mathcal{L}(\mathcal{G}) + K)\tilde{\gamma}(t) \\ &\quad - \tau_\gamma \mathrm{sgn}\Big[ (\mathcal{L}(\mathcal{G}) + K)\tilde{\gamma}(t) \Big] - \mathbf{1}_n \dot{\gamma}(t) \bigg) \\ &\leq -\tilde{\gamma}^T(\mathcal{L}(\mathcal{G}) + K)^2 \tilde{\gamma}(t) - \tau_\gamma \|(\mathcal{L}(\mathcal{G}) + K)\tilde{\gamma}(t)\|_1 \\ &\quad + |\dot{\gamma}(t)| \|(\mathcal{L}(\mathcal{G}) + K)\tilde{\gamma}(t)\|_1 \\ &\leq -\tilde{\gamma}^T(\mathcal{L}(\mathcal{G}) + K)^2 \tilde{\gamma}(t) \\ &\quad - (\tau_\gamma - \omega_\gamma)\|(\mathcal{L}(\mathcal{G}) + K)\tilde{\gamma}(t)\|_1. \quad (11)\end{aligned}$$

Since $\mathcal{L}(\mathcal{G}) + K \in \mathbb{R}_+^{n \times n}$ [Lemma 2, 32] and $(\tau_\gamma - \omega_\gamma) > 0$, $\dot{V}(\tilde{\gamma}(t))$ is negative definite. As a result, from Theorem 3.1 of [33], $\lim_{t \to \infty} \tilde{\gamma}_i(t) = 0$, and with the same analysis, $\lim_{t \to \infty} \tilde{\theta}_i(t) = 0$ hold for all $i = 1, \dots, n$. This implies that $\gamma_i(t) \to \gamma(t)$ and $\theta_i(t) \to \theta(t)$ as $t \to \infty$ for all $i = 1, \dots, n$. Hence, it now readily follows from the limit properties along with the squeeze theorem [34] that $R(\theta_i(t)) \to R(\theta(t))$ as $t \to \infty$, where this further implies that $\gamma_i(t)R(\theta_i(t)) \to \gamma(t)R(\theta(t))$ as $t \to \infty$ for all $i = 1, \dots, n$.

Next, we prove that under the main layer (2), agents reach consensus, and (6) will be achieved. Consider the state transformation given by $\tilde{x}_i(t) \triangleq x_i(t) - \gamma_i(t)R(\theta_i(t))\xi_i$, $i = 1, \dots, n$. Using this state transformation with (2) yields

$$\dot{\tilde{x}}_i(t) = - \sum_{j \in \mathcal{N}_i^f} \big( \tilde{x}_i(t) - \tilde{x}_j(t) \big). \quad (12)$$

By letting $\tilde{x}(t) \triangleq \big[\tilde{x}_1(t), \dots, \tilde{x}_n(t)\big]^{\mathrm{T}}$, (12) can be written in a compact form as

$$\dot{\tilde{x}}(t) = -\big(\mathcal{L}(\mathcal{G}) \otimes \mathrm{I}_2\big)\tilde{x}(t), \quad (13)$$

and therefore, $\lim_{t \to \infty} [\tilde{x}_i(t)]_k = \big([\tilde{x}_1(0)]_k + \cdots [\tilde{x}_n(0)]_k\big)/n$ holds for $i = 1, \dots, n$ and $k = 1, 2$. As a consequence, $x_i(t) - x_j(t) \to \gamma_i(t)R(\theta_i(t))\xi_i - \gamma_j(t)R(\theta_j(t))\xi_j$ as $t \to \infty$ for all $i = 1, \dots, n$ and $j \in N_i^f$. Finally, from $x_i(t) - x_j(t) \to \gamma_i(t)R(\theta_i(t))\xi_i - \gamma_j(t)R(\theta_j(t))\xi_j$ as $t \to \infty$ and $\gamma_i(t)R(\theta_i(t)) \to \gamma(t)R(\theta(t))$ as $t \to \infty$, one can conclude that $x_i(t) - x_j(t) \to \gamma(t)R\big(\theta(t)\big)\big(\xi_i - \xi_j\big)$ as $t \to \infty$ using the limit properties, where the result is now immediate. ∎

**Remark 1.** Theorem 1 shows that the proposed algorithm given by (2), (3) and (4) allows size and orientation of the multiagent formation to be controlled by formation size parameter $\gamma(t)$ and orientation parameter $\theta(t)$, which are only available to capable agents (not globally).

**Remark 2.** The dynamical structure of the two underlying layers (3) and (4) uses the signum functions in order to achieve asymptotic stability in the presence of time-varying signals $\gamma(t)$ and $\theta(t)$, where such functions are also adopted in the networked multiagent systems literature (see, for example, [31], [35]). Note that if $\gamma(t)$ and $\theta(t)$ are constants, then the results of Theorem 1 still hold without the need for the signum function in (3) and (4); that is,

$$\dot{\gamma}_i(t) = - \sum_{j \in \mathcal{N}_i^f} \big(\gamma_i(t) - \gamma_j(t)\big) - k_i\big(\gamma_i(t) - \gamma(t)\big),$$
$$\gamma_i(0) = \gamma_{i0}, \quad (14)$$

$$\dot{\theta}_i(t) = - \sum_{j \in \mathcal{N}_i^f} \big(\theta_i(t) - \theta_j(t)\big) - k_i\big(\theta_i(t) - \theta(t)\big),$$
$$\theta_i(0) = \theta_{i0}. \quad (15)$$

**Remark 3.** For improving the rate of convergence of the networked multiagent system, without loss of generality, we can introduce a positive parameter $\alpha$ to the main layer (2) as

$$\begin{aligned}\dot{x}_i(t) = \alpha\Big[ &- \sum_{j \in \mathcal{N}_i^f} \big( x_i(t) - x_j(t) \big) \\ &+ \sum_{j \in \mathcal{N}_i^f} \Big( \gamma_i(t)R(\theta_i(t))\xi_i - \gamma_j(t)R(\theta_j(t))\xi_j \Big) \Big] \\ &+ \dot{\gamma}_i(t)R(\theta_i(t))\xi_i + \gamma_i(t)\dot{R}(\theta_i(t))\xi_i, \quad x_i(0) = x_{i0}, \end{aligned}$$
$$(16)$$

**Remark 4.** The proposed algorithm in Theorem 1 can be extended to a three dimensional case with $x_i(t) \in \mathbb{R}^3$. In this case, the rotation matrix becomes

$$R\big(\theta_i^x(t), \theta_i^y(t), \theta_i^z(t)\big) = R_x\big(\theta_i^x(t)\big)R_y\big(\theta_i^y(t)\big)R_z\big(\theta_i^z(t)\big), \quad (17)$$

where $\theta_i^x(t) \in \mathbb{R}$, $\theta_i^y(t) \in \mathbb{R}$, and $\theta_i^z(t) \in \mathbb{R}$ are the rotation angles corresponding to yaw, pitch, and roll, respectively. Also, instead of using only one layer for $\theta_i(t)$ like in 2D case, we now need three layers for $\theta_i^x(t)$, $\theta_i^y(t)$, and $\theta_i^z(t)$.

**Remark 5.** The proposed multiplex networks-based spatial formation control algorithm given by (2), (3) and (4) can be also extended to the case where the graph $\mathcal{G}$ is directed under the assumption that there exists at least one capable agent at the root of the spanning tree [2].

**Remark 6.** The communication graph topologies for (2), (3), and (4) can be different as long as they are undirected and connected graphs.
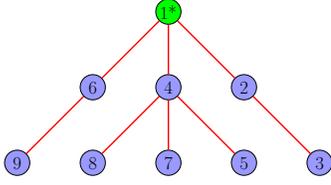
Fig. 1: A given desired formation for the example in Section III.B.

### B. Illustrative Numerical Example

We now consider a group of 9 agents with agent 1 being a capable agent and assign random initial conditions to agents. For the invariant formation problem described earlier, we choose $\xi_i$ of each agent to obtain a formation depicted in Figure 1 (in this figure, solid lines represent an undirected information exchange between agents). To control both the size and the orientation of the multiagent formation depicted in Figure 1, we use the algorithm given by (2), (3) and (4) with $(\gamma, \theta) = (0.8, -\pi/2)$, $(\gamma, \theta) = (1.0, \pi/3)$, $(\gamma, \theta) = (2.0, \pi/6)$ in Figures 2(a), 2(b), and 2(c), respectively. As expected from the results discussed in Section III.A, the resulting formation in these figures have different sizes and orientations controlled locally through the formation size and orientation parameters $(\gamma, \theta)$ available to the capable agent.

## IV. SPATIALLY EVOLVING MULTIAGENT FORMATION TRACKING

In this section, we generalize the results from the previous section to formation tracking problem in order to control the size and orientation of the formation while tracking a dynamic target (Section IV.A). The algorithms are then further extended to allow connectivity maintenance and collision avoidance (Section IV.B). A numerical example is presented to illustrate the efficacy of the methods (Section IV.C).

### A. Multiagent Formation Tracking through Multiplex Information Networks

Consider a system of $n$ agents exchanging information among each other using their local measurements according to a connected, undirected graph $\mathcal{G}$. Specifically, we propose a distributed control architecture using networks having multiple layers with the main (physical) network layer given by

$$
\begin{aligned}
\dot{x}_i(t) = & -\sum_{j \in \mathcal{N}_i^f} \Big( \big(x_i(t) - p_i(t) - c_i(t)\big) \\
& - \big(x_j(t) - p_j(t) - c_j(t)\big)\Big) \\
& - k_i\big(x_i(t) - p_i(t) - c_i(t)\big) + \dot{p}_i(t) + \dot{c}_i(t), \\
& \hspace{4cm} x_i(0) = x_{i0}, \quad (18)
\end{aligned}
$$

where $x_i(t) \in \mathbb{R}^2$ denotes the state (i.e., physical position) of agent $i$, and $c_i(t) \triangleq [c_i^x(t), c_i^y(t)]^T \in \mathbb{R}^2$ and

$$
p_i(t) \triangleq R\big(\theta_i(t)\big) S\big(\gamma_i^x(t), \gamma_i^y(t)\big) \xi_i \in \mathbb{R}^2, \quad (19)
$$

correspond to the signals locally obtained through other network layers described in the next paragraph. In (18), $k_i = 1$ only for capable agents and it is zero otherwise. Note that we implicitly assume that there exists at least one capable agent in the multiagent system. In (19), $\xi_i \in \mathbb{R}^2$ denotes the original formation shape of agent $i$ in the sense discussed in Section
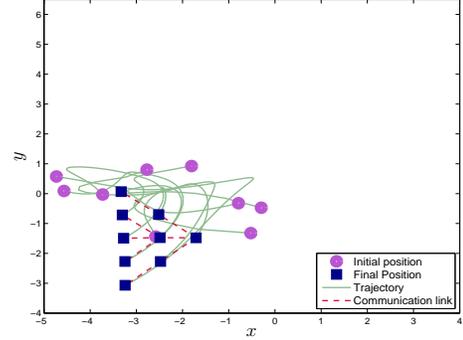


(a) $\gamma = 0.8$, $\theta = -\pi/2$
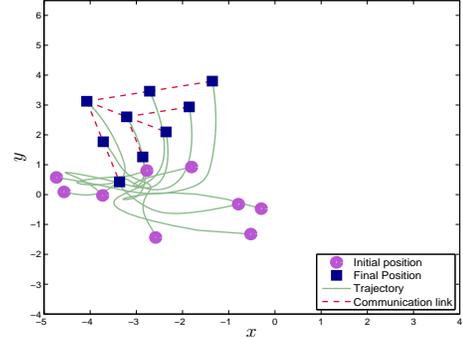


(b) $\gamma = 1.0$, $\theta = \pi/3$
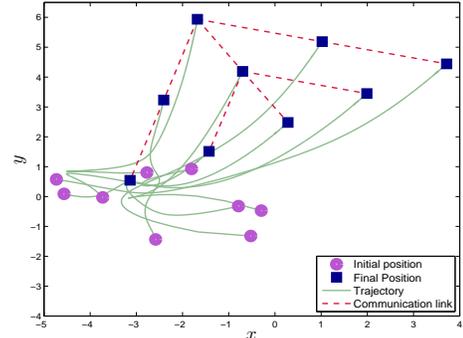


(c) $\gamma = 2.0$, $\theta = \pi/6$

Fig. 2: Formation size and orientation control using the results in Theorem 1 for different $(\gamma, \theta)$ pairs.

II.B, $\theta_i(t) \in \mathbb{R}$ is the rotation angle of agent $i$ that is used in its local rotation matrix given by (5), and $\gamma_i^x(t) \in \mathbb{R}$ and $\gamma_i^y(t) \in \mathbb{R}$ are scaling factors of agent $i$ in $x$ and $y$ dimensions of the planar space, respectively, that are used in its local scaling matrix given by

$$
S\big(\gamma_i^x(t), \gamma_i^y(t)\big) \triangleq \mathrm{diag}\big([\gamma_i^x(t), \gamma_i^y(t)]^T\big) \in \mathbb{R}^{2 \times 2}. \quad (20)
$$

To define the dynamical structure of other network layers, let $\phi_i(t)$ denotes either $c_i^x(t) \in \mathbb{R}$, $c_i^y(t) \in \mathbb{R}$, $\theta_i(t) \in \mathbb{R}$, $\gamma_i^x(t) \in \mathbb{R}$, or $\gamma_i^y(t) \in \mathbb{R}$ for conciseness of the following discussion that satisfy

$$
\dot{\phi}_i(t) = -q_i(t) - \tau \mathrm{sgn}\big(q_i(t)\big), \ \phi_i(0) = \phi_{i0}, \quad (21)
$$

$$
q_i(t) \triangleq \sum_{j \in \mathcal{N}_i^f} \big(\phi_i(t) - \phi_j(t)\big) + k_i\big(\phi_i(t) - \phi_0(t)\big), (22)
$$

where $\tau \in \mathbb{R}$ is a positive design parameter and it is assumed

that $\phi_0(t)$ and $\dot{\phi}_0(t)$ are bounded. Note that in (21) and (22), $\phi_0(t)$ denotes either $c^x(t) \in \mathbb{R}$, $c^y(t) \in \mathbb{R}$, $\theta_0(t) \in \mathbb{R}$, $\gamma_0^x(t) \in \mathbb{R}$, or $\gamma_0^y(t) \in \mathbb{R}$, where $c(t) \triangleq [c^x(t), c^y(t)]^{\mathrm{T}}$ is the position of the dynamic target on a planar space, $\theta_0(t)$ is the desired rotation angle, and $\gamma_0^x(t)$ and $\gamma_0^y(t)$ are desired scaling factors, respectively. Since $k_i = 1$ only for capable agents, $c(t)$, $\theta_0(t)$, $\gamma_0^x(t)$, and $\gamma_0^y(t)$ are only available to these capable agents.

Since $\dot{\phi}_0(t)$ is bounded, this implies that $|\dot{c}^x(t)| \leq \omega_{c^x}$, $|\dot{c}^y(t)| \leq \omega_{c^y}$, $|\dot{\theta}_0(t)| \leq \omega_{\theta_0}$, $|\dot{\gamma}_0^x(t)| \leq \omega_{\gamma_0^x}$, and $|\dot{\gamma}_0^y(t)| \leq \omega_{\gamma_0^y}$. In what follows, we let $\omega$ to be the largest constant among $\omega_{c^x}$, $\omega_{c^y}$, $\omega_{\theta_0}$, $\omega_{\gamma_0^x}$, and $\omega_{\gamma_0^y}$ without loss of generality (i.e., $|\dot{\phi}_0(t)| \leq \omega$), and set $\tau > \omega$. The next theorem presenting the second result of this paper shows that the multiplex information networks-based distributed controller architecture given by (18) and (21) not only allows agents to track a dynamic target but also allows them to alter size and orientation of the resulting formation.

**Theorem 2.** Consider the networked multiagent system given by (18) and (21), where agents exchange their local measurements using an undirected and connected graph $\mathcal{G}$. Then, the expression given by

$$\lim_{t \to \infty} \left( x_i(t) - \rho_i(t) \right) = 0, \tag{23}$$

holds for all $i = 1, \ldots, n$, where $\rho_i(t) \triangleq c(t) + R\big(\theta_0(t)\big)S\big(\gamma_0^x(t), \gamma_0^y(t)\big)\xi_i$.

*Proof.* We first show that $\phi_i(t)$ converges to $\phi_0(t)$ for all cases when $\phi_i(t)$ denotes either $c_i(t) \in \mathbb{R}^2$, $\theta_i(t) \in \mathbb{R}$, $\gamma_i^x(t) \in \mathbb{R}$, or $\gamma_i^y(t) \in \mathbb{R}$. For this purpose, consider the state transformation given by $\tilde{\phi}_i(t) \triangleq \phi_i(t) - \phi_0(t)$, $i = 1, \ldots, n$. Using this state transformation with (21) and (22) yields

$$\dot{\tilde{\phi}}_i(t) = -q_i(t) - \tau \mathrm{sgn}\big(q_i(t)\big) - \dot{\phi}_0(t), \tag{24}$$

$$q_i(t) = \sum_{j \in \mathcal{N}_i^f} \big(\tilde{\phi}_i(t) - \tilde{\phi}_j(t)\big) + k_i \tilde{\phi}_i(t). \tag{25}$$

By letting $\tilde{\phi}(t) \triangleq [\tilde{\phi}_1(t), \ldots, \tilde{\phi}_n(t)]^T$, (24) and (25) can be written in the compact form as

$$\dot{\tilde{\phi}}(t) = -q(t) - \tau \mathrm{sgn}\big(q(t)\big) - \mathbf{1}_n \dot{\phi}_0(t), \tag{26}$$

$$q(t) = \big(\mathcal{L}(\mathcal{G}) + K\big)\tilde{\phi}(t), \tag{27}$$

where $K \triangleq \mathrm{diag}([k_1, \ldots, k_n]^T)$. Now, consider the Lyapunov function candidate $V(\tilde{\phi}) = \frac{1}{2}\tilde{\phi}^T(\mathcal{L}(\mathcal{G}) + K)\tilde{\phi}$, where its time derivative along the trajectory of (26) is given by

$$\dot{V}(\tilde{\phi}(t)) = \tilde{\phi}^T(\mathcal{L}(\mathcal{G}) + K)\bigg( -(\mathcal{L}(\mathcal{G}) + K)\tilde{\phi}(t)$$
$$-\tau \mathrm{sgn}\Big[(\mathcal{L}(\mathcal{G}) + K)\tilde{\phi}(t)\Big] - \mathbf{1}_n \dot{\phi}_0(t) \bigg)$$
$$\leq -\tilde{\phi}^T(\mathcal{L}(\mathcal{G}) + K)^2\tilde{\phi}(t) - \tau\|(\mathcal{L}(\mathcal{G}) + K)\tilde{\phi}(t)\|_1$$
$$+|\dot{\phi}_0(t)|\|(\mathcal{L}(\mathcal{G}) + K)\tilde{\phi}(t)\|_1$$
$$\leq -\tilde{\phi}^T(\mathcal{L}(\mathcal{G}) + K)^2\tilde{\phi}(t)$$
$$-(\tau - \omega)\|(\mathcal{L}(\mathcal{G}) + K)\tilde{\phi}(t)\|_1. \tag{28}$$

Since $\mathcal{L}(\mathcal{G}) + K \in \mathbb{R}_+^{n \times n}$ [Lemma 2, 32] and $(\tau - \omega) > 0$ by definition, $\dot{V}(\tilde{\phi}(t))$ is negative definite. Therefore, from Theorem 3.1 of [33], $\tilde{\phi} \to 0$ as $t \to \infty$; or equivalently,

$\phi_i(t) \to \phi_0(t)$ as $t \to \infty$. It now readily follows from the limit properties along with the squeeze theorem [34] that $p_i(t) \to R(\theta_0(t))S(\gamma_0^x(t), \gamma_0^y(t))\xi_i$, and $c_i(t) \to c(t)$ as $t \to \infty$; hence, $c_i(t) + p_i(t) \to \rho_i(t)$ as $t \to \infty$.

Next, for the main network layer (18), let's consider the state transformation

$$z_i(t) \triangleq x_i(t) - p_i(t) - c_i(t), \quad i = 1, \ldots, n. \tag{29}$$

Using (29), (18) can be rewritten as $\dot{z}_i(t) = -\sum_{j \in \mathcal{N}_i^f}\big(z_i(t) - z_j(t)\big) - k_i z_i(t)$. Define $z(t) \triangleq [z_1(t), \ldots, z_n(t)]^T$, then the last expression can be written in the compact form as

$$\dot{z}(t) = -\big((\mathcal{L}(\mathcal{G}) + K) \otimes \mathrm{I}_2\big)z(t), \tag{30}$$

Since it is assumed that there exists at least one capable agent in the network (i.e, at least one of the diagonal elements of $K$ is equal to 1), it follows that $\mathcal{L}(\mathcal{G}) + K \in \mathbb{R}_+^{n \times n}$, and hence, $-\big(\mathcal{L}(\mathcal{G}) + K\big)$ is a Hurwitz matrix. As a direct consequence, $z(t) \to 0$ as $t \to \infty$; thus, $x_i(t) \to p_i(t) + c_i(t)$. Hence, using the limit properties, (23) holds and proof is now complete. ∎

**Remark 7.** Theorem 2 shows that under the proposed algorithm given by (18) and (21), $\lim_{t \to \infty}\big(\big(x_i(t) - x_j(t)\big) - \big(p_i(t) - p_j(t)\big)\big) = \lim_{t \to \infty}\big(\big(x_i(t) - x_j(t)\big) - R(\theta_0(t))S(\gamma_0^x(t), \gamma_0^y(t))(\xi_i - \xi_j)\big) = 0$ holds; that is, agents has formed the desired formation. Note that (23) also implies that each agent is translating a distance $c(t)$ or the formation is tracking the target.

**Remark 8.** Similar to Remark 2, if $c^x(t)$, $c^y(t)$, $\theta_0(t)$, $\gamma_0^x(t)$, and $\gamma_0^y(t)$ are constants, then Theorem 2's results still hold without the need for signum function in (21) and (22); i.e.,

$$\dot{\phi}_i(t) = -\sum_{j \in \mathcal{N}_i^f}\big(\phi_i(t) - \phi_j(t)\big) - k_i\big(\phi_i(t) - \phi_0\big). \tag{31}$$

We can also reach a similar conclusion for the case when some of these signals are constant and the respective signum functions for those are removed from (21) and (22).

**Remark 9.** Similar to Remark 3, a positive design parameter $\alpha$ can be used in the main network layer given by (18) as

$$\dot{x}_i(t) = \alpha\Big[ -\sum_{j \in \mathcal{N}_i^f}\Big(\big(x_i(t) - p_i(t) - c_i(t)\big)$$
$$-\big(x_j(t) - p_j(t) - c_j(t)\big)\Big) - k_i\big(x_i(t) - p_i(t) - c_i(t)\big)\Big]$$
$$+\dot{p}_i(t) + \dot{c}_i(t), \quad x_i(0) = x_{i0}, \tag{32}$$

in order to improve convergence rate of the networked multiagent system. In this case, the proof of Theorem 2 remains identical with the term $(\mathcal{L}(\mathcal{G}) + K)$ replaced with $\alpha(\mathcal{L}(\mathcal{G}) + K)$ in (30). We can also reach a similar conclusion when another positive design parameter is introduced to the other network layers given by (21) and (22).

**Remark 10.** Similar to Remark 4, the proposed algorithm of this section can be also extended to a three dimensional case with $x_i(t) \in \mathbb{R}^3$. In this case, $p_i(t) \in \mathbb{R}^3$ can be redefined as

$$p_i(t) \triangleq R\big(\theta_i^x(t), \theta_i^y(t), \theta_i^z(t)\big)S\big(\gamma_i^x(t), \gamma_i^y(t), \gamma_i^z(t)\big)\xi_i, \tag{33}$$

where $\theta_i^x(t) \in \mathbb{R}$, $\theta_i^y(t) \in \mathbb{R}$, and $\theta_i^z(t) \in \mathbb{R}$ are the rotation angles corresponding to yaw, pitch, and roll, respectively, $R\big(\theta_i^x(t), \theta_i^y(t), \theta_i^z(t)\big)$ is the rotation matrix, $\gamma_i^x(t) \in \mathbb{R}$, $\gamma_i^y(t) \in \mathbb{R}$, and $\gamma_i^z(t) \in \mathbb{R}$ are the scaling

factors for each dimension, and $S\big(\gamma_i^x(t), \gamma_i^y(t), \gamma_i^z(t)\big) \triangleq$ diag$([\gamma_i^x(t), \gamma_i^y(t), \gamma_i^z(t)]^T)$ is the scaling matrix. In this case, $\phi_i(t)$ represents either $c_i^x(t)$, $c_i^y(t)$, $\theta_i^x(t)$, $\theta_i^y(t)$, $\theta_i^z(t)$, $\gamma_i^x(t)$, $\gamma_i^y(t)$, or $\gamma_i^z(t)$ that satisfies (21) and (22).

**Remark 11.** The proposed multiplex networks-based spatial formation control algorithm given by (18) and (21) can be also readily extended to the case where the graph $\mathcal{G}$ is directed under the assumption that there exists at least one capable agent at the root of the spanning tree [2]. A discussion similar to Remark 6 also holds for the results of this section.

*B. Multiagent Formation Tracking with Connectivity Maintenance and Collision Avoidance through Multiplex Information Networks*

In this subsection, we use tools and methods from differential potential fields (see, for example, [1], [23], [24], [36], [37] and references therein) and generalize the results of Section IV.A to allow connectivity maintenance and collision avoidance that are needed in real-world applications. For this purpose, we let each agent have a communication range as given in Figure 3. Specifically, we assume that two arbitrary agents can only exchange information if their relative distance is less than $R$, i.e., $\|x_{ij}\|_2 < R$. Furthermore, a collision region is defined as a small disk area with radius $r < d < R$ centered at agent $i$ as depicted in this figure. In the same way, we define an escape region as a ring with radius $\Delta < r < R$ also centered at agent $i$. The region within the collision region and escape region $(d < r < \Delta)$ is called free region.

In what follows, the gradient of a scalar function $f(x)$ is defined by $\nabla_x f = \frac{\partial f}{\partial x}$ with $\frac{\partial f}{\partial x}$ being a column vector as in, for example, [36] and [Section 2.4.3, 38]. We now define a (repulsive) differential potential function for the purpose of collision avoidance as

$$V_{Rij}(x_{ij}) \triangleq \begin{cases} \left(\frac{1}{\|x_{ij}\|_2^2} - \frac{1}{d^2}\right)^2 & \text{if } \|x_{ij}\|_2 \leq d, \ j \in \mathcal{N}_i, \\ 0 & \text{otherwise,} \end{cases} \quad (34)$$

where

$$\frac{\partial V_{Rij}(x_{ij})}{\partial x_i} = \begin{cases} -4\left(\frac{1}{\|x_{ij}\|_2^2} - \frac{1}{d^2}\right)\frac{x_{ij}}{\|x_{ij}\|_2^4} \\ \qquad \text{if } \|x_{ij}\|_2 \leq d, \ j \in \mathcal{N}_i, \\ 0 \qquad \text{otherwise.} \end{cases} \quad (35)$$
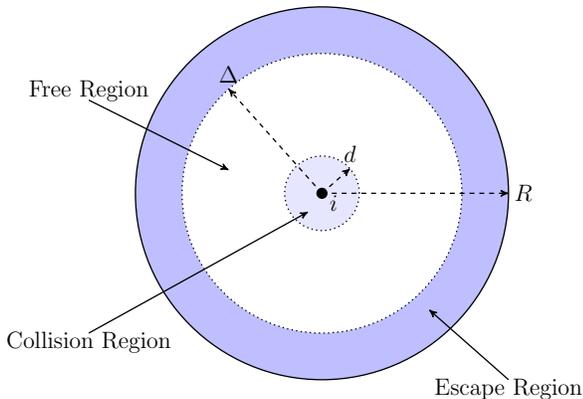
Next, we define a (attractive) differential potential function for the purpose of connectivity maintenance as

$$V_{Cij}(x_{ij}) \triangleq \begin{cases} \frac{(\|x_{ij}\|_2 - \Delta)^2}{R - \|x_{ij}\|_2} & \text{if } \|x_{ij}\|_2 \geq \Delta, \ j \in \mathcal{N}_i^f, \\ 0 & \text{otherwise,} \end{cases} \quad (36)$$

where

$$\frac{\partial V_{Cij}(x_{ij})}{\partial x_i} = \begin{cases} \frac{(\|x_{ij}\|_2 - \Delta)(2R - \Delta - \|x_{ij}\|_2)}{(R - \|x_{ij}\|_2)^2 \|x_{ij}\|_2} x_{ij} \\ \qquad \text{if } \|x_{ij}\|_2 \geq \Delta, \ j \in \mathcal{N}_i^f, \\ 0 \qquad \text{otherwise.} \end{cases} \quad (37)$$

Note that $V_{Rij} = V_{Rji}$ and $V_{Cij} = V_{Cji}$ as well as $V_{Rij} = V_{Cij} = 0$ for $i = j$. Note also that $\partial V_{Rij}(x_{ij})/\partial x_i$ and $\partial V_{Cij}(x_{ij})/\partial x_i$ defined in (35) and (37) are continuous. The repulsive differential potential function $V_{Rij}$ is smoothly activated when $\|x_{ij}\|_2 \leq d$ and grows to infinity as $\|x_{ij}\|_2$ approaches 0. In addition, the attractive differential potential function $V_{Cij}$ is smoothly activated when $\|x_{ij}\|_2 \geq \Delta$ and grows to infinity as $\|x_{ij}\|_2$ approaches $R$. Notice that $V_{Rij}$ applies to agent $i$ and any agent $j$ who are neighbor of $i$ (i.e., $j \in \mathcal{N}_i$), while $V_{Cij}$ only affects agent $i$ and its formation neighbors (i.e., $j \in \mathcal{N}_i^f$). In addition, we assume that the desired distance between any two arbitrary agents lies in the free region, where this implies that the scaling factors need to be lower and upper bounded such that this assumption is not violated.

Based on the above definitions, we generalize the results of the previous section by considering the distributed spatial formation control algorithm given by

$$\begin{aligned} \dot{x}_i(t) = & -\sum_{j \in \mathcal{N}_i^f} \Big( \big(x_i(t) - p_i(t) - c_i(t)\big) \\ & - \big(x_j(t) - p_j(t) - c_j(t)\big)\Big) \\ & - k_i\big(x_i(t) - p_i(t) - c_i(t)\big) + \dot{p}_i(t) + \dot{c}_i(t) \\ & - \sum_{j \in \mathcal{N}_i} \frac{\partial V_{Rij}(x_{ij})}{\partial x_i} - \sum_{j \in \mathcal{N}_i^f} \frac{\partial V_{Cij}(x_{ij})}{\partial x_i}, \\ & \qquad\qquad\qquad\qquad x_i(0) = x_{i0}, \quad (38) \end{aligned}$$

Since we can achieve connectivity maintenance and collision avoidance by only modifying the main network layer in (18) as (38), all other network layers given by (21) remain unchanged in this setting. The following standard assumption is necessary for the next result.

**Assumption 1.** $\partial V_{Rij}(x_{ij})/\partial x_i$ and $\partial V_{Cij}(x_{ij})/\partial x_i$ vanish over time.

The above assumption implies that the potential field $\partial V_{Rij}(x_{ij})/\partial x_i$ (resp., $\partial V_{Cij}(x_{ij})/\partial x_i$) is able to create a repulsive force (resp., an attractive force) to push two agents out of the collision region (resp., to pull two neighboring agents back to the free region with relative to each other) without causing agents to stuck in locked configurations (i.e., not being stuck in local minima). This assumption is standard in the networked multiagent systems literature that adopts tools and methods from differential potential fields (see Remark 12 below for further discussion). We further note that once two neighboring agents are in the free region with relative to each



Fig. 3: Communication range of agent $i$.

other, $\partial V_{Rij}(x_{ij})/\partial x_i$ and $\partial V_{Cij}(x_{ij})/\partial x_i$ equal to zero (i.e., they vanish by definition).

**Theorem 3.** Consider the networked multiagent system given by (38) and (21), where agents exchange their local measurements using an undirected and connected graph $\mathcal{G}$. If initially agents are connected with their formation neighbors and there is no collision, and Assumption 1 holds, then (23) holds for all $i = 1, \ldots, n$ with connectivity maintenance and collision avoidance for all $t \geq 0$.

*Proof.* Following the discussion given after (38), we first note that the other network layers represented by (21) remain unchanged in the setting of this theorem. Hence, from the first paragraph of the proof of Theorem 2, $c_i(t) + p_i(t) \to \rho_i(t)$ as $t \to \infty$ holds.

Using the state transformation given by (29), we next note that (38) can be rewritten as

$$
\dot{z}_i(t) = -\sum_{j \in \mathcal{N}_i^f} \Big( z_i(t) - z_j(t) \Big) - k_i z_i(t)
$$
$$
- \sum_{j \in \mathcal{N}_i} \frac{\partial V_{Rij}(x_{ij})}{\partial z_i} - \sum_{j \in \mathcal{N}_i^f} \frac{\partial V_{Cij}(x_{ij})}{\partial z_i}. \quad (39)
$$

Note also that $\frac{\partial V_{Rij}(x_{ij})}{\partial x_i(t)} = \frac{\partial V_{Rij}(x_{ij})}{\partial z_i(t)}$ and $\frac{\partial V_{Cij}(x_{ij})}{\partial x_i(t)} = \frac{\partial V_{Cij}(x_{ij})}{\partial z_i(t)}$. We define

$$
V_{Ai}(z(t)) \triangleq \frac{1}{2} \sum_{j \in \mathcal{N}_i^f} \|z_i(t) - z_j(t)\|_2^2 + \frac{1}{2} k_i \|z_i(t)\|_2^2, \quad (40)
$$

where the partial derivative of (40) with respect to $z_i(t)$ is given by $\frac{\partial V_{Ai}(z(t))}{\partial z_i(t)} = \sum_{j \in \mathcal{N}_i^f} \Big( z_i(t) - z_j(t) \Big) + k_i z_i(t)$. Now, we can write

$$
\dot{z}_i(t) = -\frac{\partial V_{Ai}(z(t))}{\partial z_i(t)} - \sum_{j \in \mathcal{N}_i} \frac{\partial V_{Rij}(x_{ij})}{\partial z_i(t)} - \sum_{j \in \mathcal{N}_i^f} \frac{\partial V_{Cij}(x_{ij})}{\partial z_i(t)}
$$
$$
= -\frac{\partial V_{Ai}(z(t))}{\partial z_i(t)} - \sum_{j=1}^n \Big( \frac{\partial V_{Rij}(x_{ij})}{\partial z_i(t)} + \frac{\partial V_{Cij}(x_{ij})}{\partial z_i(t)} \Big).
$$
$$(41)$$

Next, consider the continuously differentiable function $V : D_V \times \mathbb{R}^{2n} \to \overline{\mathbb{R}}_+$ given by

$$
V(\cdot) = \Big( \frac{1}{2} \sum_{i=1}^n V_{Ai}(z(t)) + \frac{1}{4} \sum_{i=1}^n k_i \|z_i(t)\|_2^2 \Big)
$$
$$
+ \frac{1}{2} \sum_{i=1}^n \sum_{j=1}^n \Big( V_{Rij}(x_{ij}) + V_{Cij}(x_{ij}) \Big), \quad (42)
$$

where $D_V = \{x \in \mathbb{R}^{2n} : \|x_{ij}\|_2 \in (0, R) \ \forall \ j \in \mathcal{N}_i^f$ and $\|x_{ij}\|_2 \in (0, \infty) \ \forall \ j \in \mathcal{N}_i \setminus \mathcal{N}_i^f \}$. For any $c > 0$, let $\Omega = \{(x, z) \in D_V \times \mathbb{R}^{2n} : V(\cdot) \leq c\}$ denote the level sets of $V(\cdot)$ and note that

$$
\dot{V}(\cdot) = \Big[ \Big( \frac{\partial V}{\partial z_1} \Big)^{\mathrm{T}} \ \ \Big( \frac{\partial V}{\partial z_2} \Big)^{\mathrm{T}} \ \ \cdots \ \ \Big( \frac{\partial V}{\partial z_n} \Big)^{\mathrm{T}} \Big] \begin{bmatrix} \dot{z}_1(t) \\ \dot{z}_2(t) \\ \vdots \\ \dot{z}_n(t) \end{bmatrix}
$$

$$
= \sum_{i=1}^n \Big( \frac{\partial V}{\partial z_i} \Big)^{\mathrm{T}} \dot{z}_i(t). \quad (43)
$$

In what follows, we show that $\frac{\partial V}{\partial z_i} = -\dot{z}_i(t)$. To this end, we first write

$$
\frac{\partial V}{\partial z_i} = \frac{\partial}{\partial z_i} \Big( \frac{1}{2} \sum_{i=1}^n V_{Ai}(z(t)) + \frac{1}{4} \sum_{i=1}^n k_i \|z_i(t)\|_2^2
$$
$$
+ \frac{1}{2} \sum_{i=1}^n \sum_{j=1}^n \Big( V_{Rij}(x_{ij}) + V_{Cij}(x_{ij}) \Big) \Big)
$$
$$
= \underbrace{\frac{1}{2} \frac{\partial}{\partial z_i} \Big( \sum_{i=1}^n V_{Ai}(z(t)) \Big)}_{A} + \underbrace{\frac{1}{4} \frac{\partial}{\partial z_i} \Big( \sum_{i=1}^n k_i \|z_i(t)\|_2^2 \Big)}_{B}
$$
$$
+ \underbrace{\frac{1}{2} \frac{\partial}{\partial z_i} \Big( \sum_{i=1}^n \sum_{j=1}^n \Big( V_{Rij}(x_{ij}) + V_{Cij}(x_{ij}) \Big) \Big)}_{C}, \quad (44)
$$

where

$$
A = \frac{1}{2} \frac{\partial}{\partial z_i} \Big( V_{A1}(z(t)) + V_{A2}(z(t)) + \ldots + V_{An}(z(t)) \Big)
$$
$$
= \frac{1}{2} \frac{\partial V_{A1}(z(t))}{\partial z_i} + \frac{1}{2} \frac{\partial V_{A2}(z(t))}{\partial z_i} + \ldots + \frac{1}{2} \frac{\partial V_{An}(z(t))}{\partial z_i}
$$
$$
= \frac{1}{2} \frac{\partial V_{Ai}(z(t))}{\partial z_i} + \frac{1}{2} \sum_{j=1, \ j \neq i}^n \Big( \frac{\partial V_{Aj}(z(t))}{\partial z_i} \Big). \quad (45)
$$

Note that if $i \notin \mathcal{N}_j^f$ then $\frac{\partial V_{Aj}(z(t))}{\partial z_i} = 0$ and if $i \in \mathcal{N}_j^f$ then

$$
\frac{\partial V_{Aj}(z(t))}{\partial z_i} = \frac{\partial}{\partial z_i} \Big( \frac{1}{2} \sum_{k \in \mathcal{N}_j^f} \|z_j(t) - z_k(t)\|_2^2 + \frac{1}{2} k_j \|z_j(t)\|_2^2 \Big)
$$
$$
= -\big( z_j(t) - z_i(t) \big) = \big( z_i(t) - z_j(t) \big), \quad (46)
$$

with respect to agents $i$ and $j$ only. This implies that we graphwise have

$$
A = \frac{1}{2} \frac{\partial V_{Ai}(z(t))}{\partial z_i} + \frac{1}{2} \sum_{j \in \mathcal{N}_i^f} \big( z_i(t) - z_j(t) \big). \quad (47)
$$

Furthermore, we have

$$
B = \frac{k_i}{4} \frac{\partial}{\partial z_i} \big( \|z_i(t)\|_2^2 \big) = \frac{k_i z_i(t)}{2}. \quad (48)
$$

Finally, by symmetry of the function $V_{Rij}$ and $V_{Cij}$, we have

$$
C = \frac{1}{2} \Big( 2 \sum_{j=1}^n \Big( \frac{\partial V_{Rij}(x_{ij})}{\partial z_i(t)} + \frac{\partial V_{Cij}(x_{ij})}{\partial z_i(t)} \Big) \Big)
$$
$$
= \sum_{j=1}^n \Big( \frac{\partial V_{Rij}(x_{ij})}{\partial z_i(t)} + \frac{\partial V_{Cij}(x_{ij})}{\partial z_i(t)} \Big). \quad (49)
$$

Substituting (47), (48), and (49) back into (44) yields

$$
\frac{\partial V}{\partial z_i} = \frac{1}{2} \frac{\partial V_{Ai}(z(t))}{\partial z_i} + \frac{1}{2} \sum_{j \in \mathcal{N}_i^f} \big( z_i(t) - z_j(t) \big) + \frac{k_i z_i(t)}{2}
$$
$$
+ \sum_{j=1}^n \Big( \frac{\partial V_{Rij}(x_{ij})}{\partial z_i(t)} + \frac{\partial V_{Cij}(x_{ij})}{\partial z_i(t)} \Big)
$$

$$= \frac{1}{2}\frac{\partial V_{Ai}(z(t))}{\partial z_i} + \frac{1}{2}\frac{\partial V_{Ai}(z(t))}{\partial z_i}$$
$$+ \sum_{j=1}^{n}\left(\frac{\partial V_{Rij}(x_{ij})}{\partial z_i(t)} + \frac{\partial V_{Cij}(x_{ij})}{\partial z_i(t)}\right)$$
$$= \frac{\partial V_{Ai}(z(t))}{\partial z_i} + \sum_{j=1}^{n}\left(\frac{\partial V_{Rij}(x_{ij})}{\partial z_i(t)} + \frac{\partial V_{Cij}(x_{ij})}{\partial z_i(t)}\right)$$
$$= -\dot{z}_i(t), \tag{50}$$

where the second equality comes from the expression $\frac{\partial V_{Ai}(z(t))}{\partial z_i(t)} = \sum_{j\in\mathcal{N}_i^f}\left(z_i(t) - z_j(t)\right) + k_i z_i(t)$ given in the paragraph after (40). Thus, (43) now becomes

$$\dot{V}(\cdot) = \sum_{i=1}^{n} -\dot{z}_i^{\mathrm{T}}(t)\dot{z}_i(t)$$
$$= \sum_{i=1}^{n} -\|\dot{z}_i(t)\|_2^2 \le 0. \tag{51}$$

Since $\dot{V}(\cdot) \le 0$, the level sets $\Omega$ are positively invariant, and hence, $V_{Ai}(z(t))$, $V_{Rij}(x_{ij})$ and $V_{Cij}(x_{ij})$ are bounded [36]. If for some $j \in \mathcal{N}_i$ such that $\|x_{ij}\|_2 \to 0$, then $V_{Rij} \to \infty$. Therefore, by the continuity of $V$ in $D_V$, it follows that $\|x_{ij}\|_2 > 0$ for all $j \in \mathcal{N}_i(t)$. Likewise, if for some $j \in \mathcal{N}_i^f$ such that $\|x_{ij}\|_2 \to R$, then $V_{Cij} \to \infty$. Once again, by the continuity of $V$ in $D_V$, it follows that $\|x_{ij}\|_2 < R$ for all $j \in \mathcal{N}_i^f$. Thus, if the agents are initially connected with their formation neighbors and there is no collision, then collision avoidance between agent $i$ and its neighbors (i.e., $j \in \mathcal{N}_i$) and connectivity maintenance between agent $i$ and its formation neighbors (i.e., $j \in \mathcal{N}_i^f$) are guaranteed for all $t \ge 0$.

The level sets $\Omega$ are closed by the continuity of $V$ in $D_V$ and they are bounded since $\dot{V}(\cdot) \le 0$, and hence, they are compact. By LaSalle's invariance principle, all trajectories starting in $\Omega$ converge to the largest invariant set in $E \triangleq \{(x,z) \in D_V \times \mathbb{R}^{2n} : \dot{V}(\cdot) = 0\} = \{(x,z) \in D_V \times \mathbb{R}^{2n} : \dot{z}(t) = 0\}$. From (41), this implies that $\frac{\partial V_{Ai}(z(t))}{\partial z_i(t)} = -\sum_{j=1}^{n}\left(\frac{\partial V_{Ri}(x_{ij})}{\partial z_i(t)} + \frac{\partial V_{Ci}(x_{ij})}{\partial z_i(t)}\right)$ holds. From Assumption 1 (i.e., the agents are not stuck in local minima), the term $-\sum_{j=1}^{n}\left(\frac{\partial V_{Ri}(x_{ij})}{\partial z_i(t)} + \frac{\partial V_{Ci}(x_{ij})}{\partial z_i(t)}\right)$ vanishes over time. Thus, trajectories starting in $\Omega$ converge to $M \subset E$ defined by $M \triangleq \{(x,z) \in D_V \times \mathbb{R}^{2n} : \frac{\partial V_{Ai}(z(t))}{\partial z_i(t)} = -\sum_{j=1}^{n}\left(\frac{\partial V_{Ri}(x_{ij})}{\partial z_i(t)} + \frac{\partial V_{Ci}(x_{ij})}{\partial z_i(t)}\right) = 0 \,\forall\, i = 1,\ldots,n\}$. Finally, analyzing $\frac{\partial V_{Ai}(z(t))}{\partial z_i(t)} = 0 \,\forall\, i = 1,\ldots,n$ now follows from the second paragraph of the proof of Theorem 2 owing to the fact that $\frac{\partial V_{Ai}(z(t))}{\partial z_i(t)} = \sum_{j\in\mathcal{N}_i^f}\left(z_i(t) - z_j(t)\right) + k_i z_i(t)$, where the right hand side of this expression was used there. In other words, the largest invariant set of $M$ is trivial in this case and equals to $z_i(t) = 0$ for all $i = 1,\ldots,n$ from the proof of Theorem 2. Thus, from the discussion given in the last part of Theorem 2's proof, $x_i(t) \to p_i(t) + c_i(t)$ as $t \to \infty$. Recalling the fact that the other network layers represented by (21) remain unchanged once again, $\phi_i(t) \to \phi_0(t)$ as $t \to \infty$ or $c_i(t) + p_i(t) \to \rho_i(t)$ as $t \to \infty$ from the first paragraph of the proof of Theorem 2. Hence, (23) holds by the limit properties. ∎

**Remark 12.** Without the assumption that agents are not

stuck in local minima (i.e., Assumption 1), one of the following two cases occurs based on the discussion given in the last paragraph of Theorem 3's proof:

*i)* Agents can converge to the free region and (23) holds.

*ii)* It follows from LaSalle's invariance principle and (41) that $\frac{\partial V_{Ai}(z(t))}{\partial z_i(t)} = -\sum_{j=1}^{n}\left(\frac{\partial V_{Ri}(x_{ij})}{\partial z_i(t)} + \frac{\partial V_{Ci}(x_{ij})}{\partial z_i(t)}\right)$ holds, where both left and right hand sides of this equation are not equal to zero.

Note that the latter case implies that agents are stuck in local minima. Although there are several methods to avoid local minima (see, for example, [39]–[41]), it is an open problem in the networked multiagent systems literature that adopts tools and methods from differential potential fields. Yet, for example, one can use the idea stated in [39], which assumes that agents that are stuck can be detected (e.g., agents that are not moving for a specific amount of time) and a virtual force

$$F_{vi} \triangleq \begin{cases} F_i & \text{if } \dot{z}_i(t) = 0 \text{ and } \frac{\partial V_{Ai}(z(t))}{\partial z_i(t)} \ne 0, \\ 0 & \text{otherwise,} \end{cases} \tag{52}$$

is generated to push such agents out of the local minima with $F_i$ being a random finite value for each agent (to preserve continuity, one can apply filtered version of this force). This force can eventually yield all agents to converge to the free region such that (23) follows.

### C. Illustrative Numerical Example

We now present a numerical example to illustrate the results of Sections IV.A and IV.B. For this purpose, consider a group of 5 agents with agent 1 being the capable agent and assume that all agents are subject to random initial conditions. We choose $\xi_i$ for each agent to obtain the desired formation depicted in Figure 4. Specifically, to illustrate the results of Theorem 2, we use (32) with $\alpha = 5$. In addition, for (21), we use $c^x(t) = t$; $c^y(t) = \sin(t)$; $\theta_0 = 0$; and low-pass filtered version of $\psi(t) = 0.5$ for $t \in [0,10)$, $\psi(t) = 0.25$ for $t \in [10,20)$, and $\psi(t) = 1$ for $t \in [20,\infty)$ for both $\gamma_0^x(t)$ and $\gamma_0^y(t)$. The time derivatives of $c_i^x(t)$, $c_i^y(t)$, $\theta_i(t)$, $\gamma_i^x(t)$, and $\gamma_i^y(t)$ are all upper bounded by 5 or a smaller constant, and hence, we set $\tau = 5$. Figure 5 shows that the considered group of agents perform target tracking while simultaneously forming, maintaining, and spatially altering their formation in time. Furthermore, Figures 6 and 7 show that $\gamma_i(t)$ converges to the desired values of the scaling factors and the state transformation variable $z_i(t)$ approaches to zero, respectively.

Next, we illustrate the results of Theorem 3. In particular, we add the potential field functions to (32) as in (38) and set $d = 0.5$, $\Delta = 6$, and $R = 8$, where all other design parameters remain the same. Figure 8 shows that the considered group of agents achieves the same level of performance as in Figure 5 while maintaining connectivity and avoiding collisions. In addition, Figure 9 shows the evolution of distances between agents during $t \in [0,5]$ seconds and illustrates collision avoidance properties of the proposed multiplex networks-based spatial formation control algorithm.

### V. MULTIAGENT FORMATION EXPERIMENTS

To justify theoretical results, proposed algorithms of this paper are implemented on a group of 3 robots. In the first
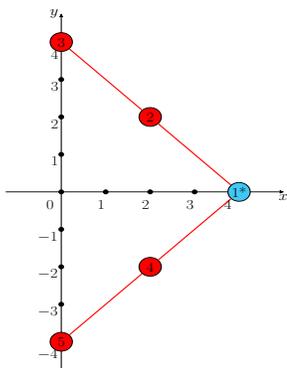
Fig. 4: A given desired formation for the example in Section IV.C.
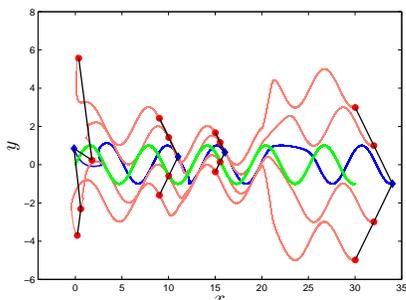


Fig. 5: Target tracking using the proposed multiplex networks-based spatial formation control algorithm in Theorem 2.
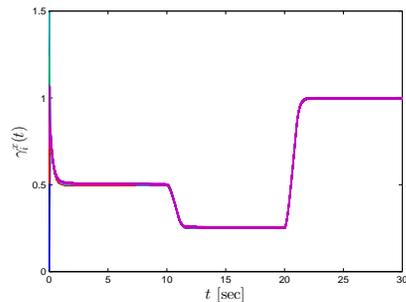


(a) Time evolution of $\gamma_i^x(t)$.
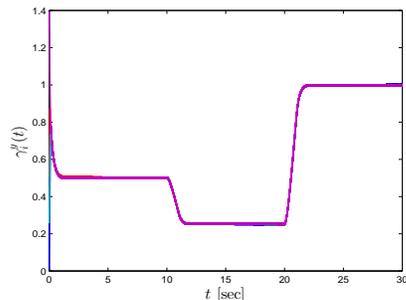


(b) Time evolution of $\gamma_i^y(t)$.

Fig. 6: Time evolution of the scaling factors in Figure 5.



(a) Time evolution of $z_i^x(t)$.



(b) Time evolution of $z_i^y(t)$

Fig. 7: Time evolution of $z_i(t)$ in Figure 5.
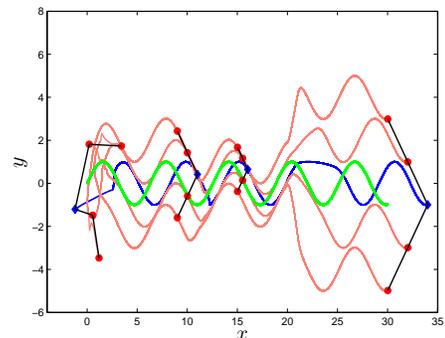


Fig. 8: Target tracking using the proposed multiplex networks-based spatial formation control algorithm in Theorem 3.
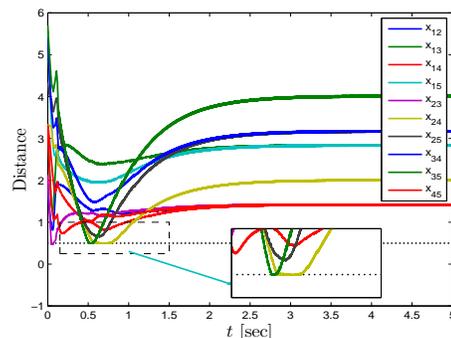


Fig. 9: Time evolution of distances between agents in Figure 8.

experiment, the robots form a V-shape formation with the size and orientation changed overtime. For the second experiment, the robots also achieve the same formation while tracking a dynamic target. In the third experiment, the robot formation is controlled to pass through a narrow passage. The mobile robot platform used in our experiments is Qbot 2 (Figure 10(a)). In addition, a motion capture system is used to detect the position

and orientation of each robot. However, each robot is limited to know only its local measurements and exchanges these data with its neighbors via a wireless network. The motion capture system is able to cover the workspace shown in Figure 10(b).

*A. Experiment 1: Formation Density and Orientation Control in Formation Assignment*

In this experiment, the robots are implemented with algorithms (2), (3) and (4). The desired scaling factor $\gamma$ and

(a) Qbot 2
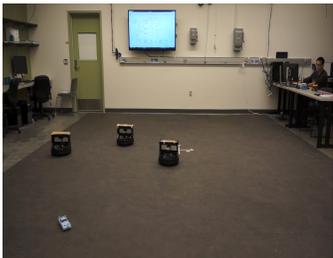


(b) Workspace

Fig. 10: Laboratory-level experimental setup.

rotation angle $\theta$ are changed by an operator from the computer station. Robot 1 is set as the capable agent, so it is the only one knows these desired values. Initially, the robots are placed randomly in the workspace. The data in Figure 11 shows that robots are able to form the formation with $(\gamma, \theta) = (1, 0)$ for $t \in [0, 36)$, $(\gamma, \theta) = (0.7, -\pi/2)$ for $t \in [36, 68)$ and $(\gamma, \theta) = (1.5, \pi/3)$ for $t \in [68, 100]$. This experiment has confirmed our Theorem 1.

### B. Experiment 2: Spatially Evolving Multiagent Formation Tracking

In this experiment, we implement algorithms (38) and (21) on the robots. The data in Figure 13 illustrates the five configurations of the robots (circles) and the target (square) over time. At t = 0, the robots are far apart from each other while the desired scaling factor is set to $\gamma = 0.7$. At t = 25, the robots are coming closer to form the desired formation and tracking the target. At t = 35, the formation is completed and following the target. As observed from the controller of Robot 1 in Figure 14, there is an impulse around t = 40. This is owing to the fact that the operator has just assigned a new scaling factor $\gamma = 1.4$ to the capable agent (i.e., robot 1). At t = 47, the formation with $\gamma = 1.4$ is achieved. At t = 62, the robots are still tracking the target while maintaining the desired formation. This experiment has confirmed our Theorem 2.

### C. Experiment 3: Formation Passing Through a Narrow Passage

We finally consider the scenario that formation has to track a target and pass through a narrow passage. With the proposed algorithms, we come up with two strategies: For the first strategy, we adjust the scaling factor $\gamma_x$ and $\gamma_y$ to make formation small enough to pass through passage as shown in Figure 15. For the second strategy, we observe that the V-shape formation (Figure 4) can be compressed to a line formation through setting the scaling factor in $x$-direction $\gamma_x = 0$. Therefore, in order to pass through the narrow passage, we
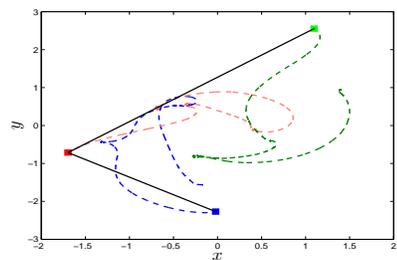


(a) $t = 0$
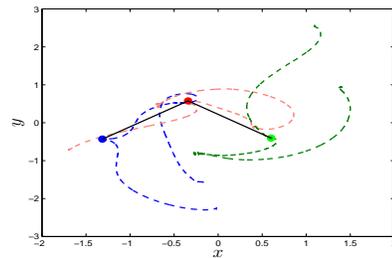


(b) $t = 35$
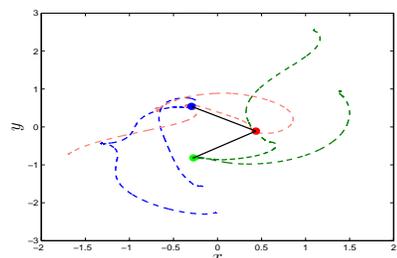


(c) $t = 67$
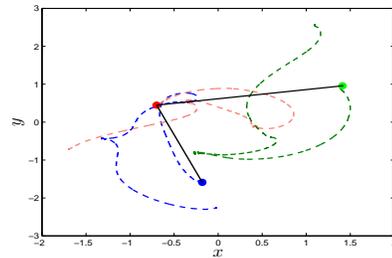


(d) $t = 100$

Fig. 11: Results of multiagent formation experiment 1.

rotate the V-shape formation by an angle $\theta = \pi/2$ and set $\gamma_y = 0$ (note that, when we rotate the formation by 90 degree, the original x-axis becomes y-axis and vice versa). The results are shown in Figure 16.

### VI. CONCLUSION

In this paper, we investigated how information exchange rules represented by multiplex information networks can be designed to enable spatially evolving multiagent formations. Specifically, we introduced, analyzed, and experimentally validated new distributed control architectures for the formation assignment (i.e., creating a desired formation for the multiagent system in hand) and the formation tracking (i.e., formation control while tracking a dynamic, non-stationary target) problems that allow capable agents to spatially alter size and orientation of the resulting formation without requiring global information exchange ability. Considering multiagent

(a) Robot 1 control history



(b) Robot 2 control history



(c) Robot 3 control history
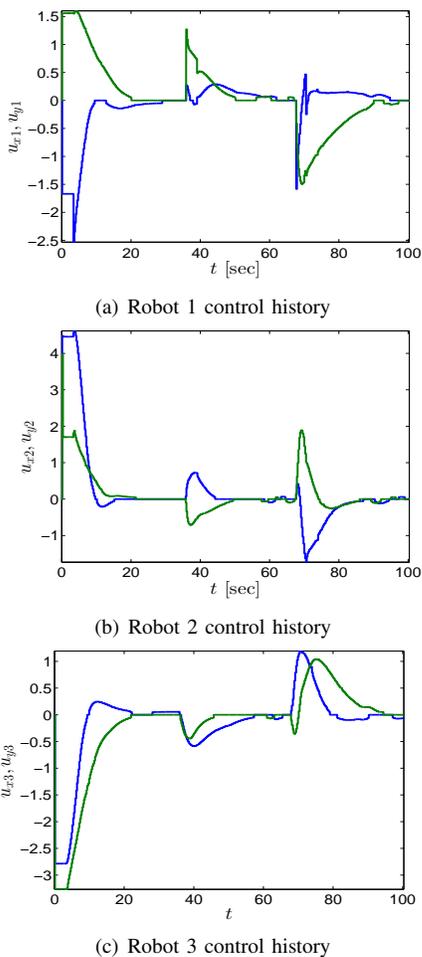
Fig. 12: Control histories of each robot for multiagent formation experiment 1.
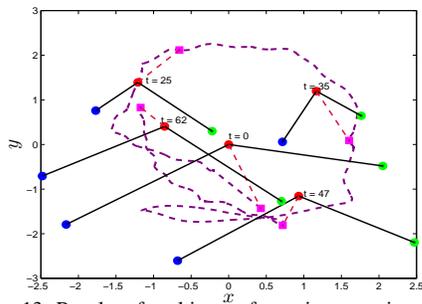


Fig. 13: Results of multiagent formation experiment 2.

operations with dramatically increasing levels of complexity, the presented multiplex networks-based approach can also be used with many other approaches in multiagent systems to enable advanced distributed information exchange rules to make these systems evolve spatially in adapting to dynamic environments and respond effectively to human interventions. Our future research will include additional theoretical developments and applications for a group of heterogeneous ground and aerial robots with exogenous disturbances, system uncertainties, and communication constraints. We will also consider the cases when the roles of capable agents switch in a given multiagent system.

## VII. ACKNOWLEDGMENTS

## REFERENCES

[1] M. Mesbahi and M. Egerstedt, *Graph theoretic methods in multiagent networks*. Princeton University Press, 2010.

[2] W. Ren and R. W. Beard, *Distributed consensus in multi-vehicle cooperative control*. Springer, 2008.

[3] K.-K. Oh and H.-S. Ahn, "A survey of formation of mobile agents," in *IEEE International Symposium on Intelligent Control*, 2010, pp. 1470–1475.

[4] P. J. Mucha, T. Richardson, K. Macon, M. A. Porter, and J.-P. Onnela, "Community structure in time-dependent, multiscale, and multiplex networks," *Science*, vol. 328, no. 5980, pp. 876–878, 2010.

[5] J. Gómez-Gardenes, I. Reinares, A. Arenas, and L. M. Floría, "Evolution of cooperation in multiplex networks," *Scientific reports*, 2012.

[6] S. Gomez, A. Diaz-Guilera, J. Gomez-Gardeñes, C. J. Perez-Vicente, Y. Moreno, and A. Arenas, "Diffusion dynamics on multiplex networks," *Physical review letters*, vol. 110, no. 2, p. 028701, 2013.

[7] M. De Domenico, A. Solé-Ribalta, E. Cozzo, M. Kivelä, Y. Moreno, M. A. Porter, S. Gómez, and A. Arenas, "Mathematical formulation of multilayer networks," *Physical Review X*, vol. 3, no. 4, p. 041022, 2013.

(a) Robot 1 control history



(b) Robot 2 control history



(c) Robot 3 control history
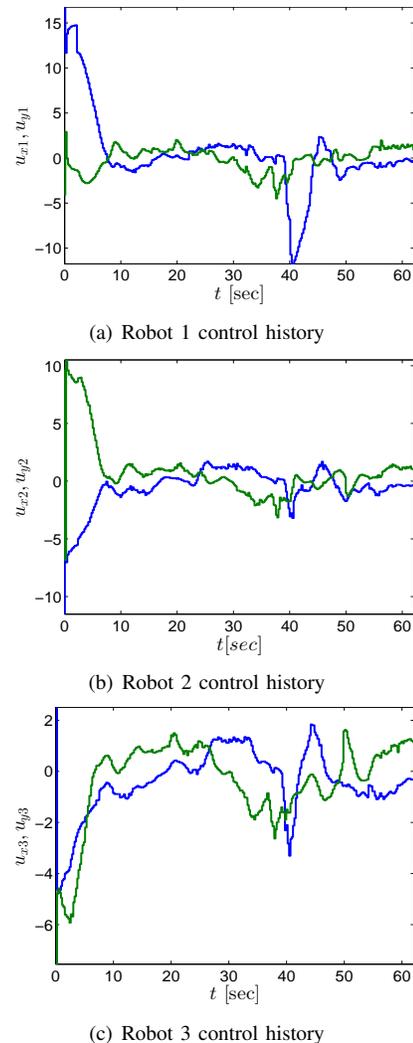
Fig. 14: Control histories of each robot for multiagent formation experiment 2.
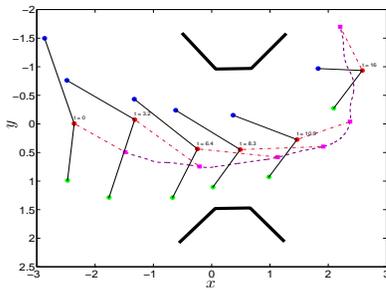
Fig. 15: Result of multiagent formation experiment 3 with the first strategy.
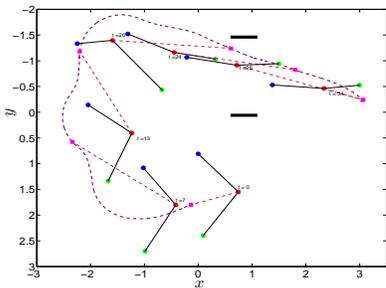


Fig. 16: Result of multiagent formation experiment 3 with the second strategy.

[8] A. Sole-Ribalta, M. De Domenico, N. E. Kouvaris, S. Gomez, and A. Arenas, "Spectral properties of the laplacian of multiplex networks," *Physical Review E*, vol. 88, no. 3, p. 032807, 2013.

[9] C. Granell, S. Gómez, and A. Arenas, "Dynamical interplay between awareness and epidemic spreading in multiplex networks," *Physical review letters*, vol. 111, no. 12, p. 128701, 2013.

[10] M. Rebollo, E. del Val, C. Carrascosa, A. Palomares, and F. Pedroche, "Consensus over multiplex network to calculate user influence in social networks," *Int. J. Complex Systems in Science*, vol. 3, no. 1, pp. 71–75, 2013.

[11] V. Nicosia and V. Latora, "Measuring and modelling correlations in multiplex networks," *arXiv preprint arXiv:1403.1546*, 2014.

[12] M. Kivelä, A. Arenas, M. Barthelemy, J. P. Gleeson, Y. Moreno, and M. A. Porter, "Multilayer networks," *arXiv preprint arXiv:1309.7233*, 2014.

[13] A. Chapman, M. Nabi-Abdolyousefi, and M. Mesbahi, "On the controllability and observability of cartesian product networks," in *IEEE Conferece on Decision and Control*, 2012, pp. 80–85.

[14] ——, "Controllability and observability of network-of-networks via cartesian products," *IEEE Transactions on Automatic Control*, vol. 59, no. 10, pp. 2668–2679, 2014.

[15] M. Asllani, D. M. Busiello, T. Carletti, D. Fanelli, and G. Planchon, "Turing instabilities on cartesian product networks," *arXiv preprint arXiv:1412.7055*, 2014.

[16] C. C. Cheah, S. P. Hou, and J. J. E. Slotine, "Region-based shape control for a swarm of robots," *Automatica*, vol. 45, no. 10, pp. 2406–2411, 2009.

[17] S. P. Hou, C.-C. Cheah, and J. Slotine, "Dynamic region following formation control for a swarm of robots," in *IEEE International Conference on Robotics and Automation*. IEEE, 2009, pp. 1929–1934.

[18] L. Brinón-Arranz, A. Seuret, and C. Canudas-de Wit, "Cooperative control design for time-varying formations of multi-agent systems," *IEEE Transactions on Automatic Control*, vol. 59, no. 8, pp. 2283–2288, 2014.

[19] S. Coogan and M. Arcak, "Scaling the size of a formation using relative position feedback," *Automatica*, vol. 48, no. 10, pp. 2677–2685, 2012.

[20] D. Tran and T. Yucelen, "Control of multiagent formations: A multiplex information networks-based approach," in *ASME Dynamic Systems and Control Conference*, 2015.

[21] D. Tran, T. Yucelen, and E. Pasiliao, "Multiplex information networks for spatially evolving multiagent formations," in *American Control Conference*, 2016, pp. 1912–1917.

[22] C. D. Godsil, G. Royle, and C. Godsil, *Algebraic graph theory*. Springer New York, 2001, vol. 207.

[23] T.-H. Cheng, Z. Kan, J. Rosenfeld, W. E. Dixon, *et al.*, "Decentralized formation control with connectivity maintenance and collision avoidance under limited and intermittent sensing," in *American Control Conference*, 2014, pp. 3201–3206.

[24] Z. Kan, L. Navaravong, J. M. Shea, E. L. Pasiliao, and W. E. Dixon, "Graph matching-based formation reconfiguration of networked agents with connectivity maintenance," *IEEE Transactions on Control of Network Systems*, vol. 2, no. 1, pp. 24–35, 2015.

[25] R. Olfati-Saber, J. A. Fax, and R. M. Murray, "Consensus and cooperation in networked multi-agent systems," *Proceedings of the IEEE*, vol. 95, no. 1, pp. 215–233, 2007.

[26] C.-L. Liu and Y.-P. Tian, "Formation control of multi-agent systems with heterogeneous communication delays," *International Journal of Systems Science*, vol. 40, no. 6, pp. 627–636, 2009.

[27] Q. Gao, A. S. Kammer, U. Zalluhoglu, and N. Olgac, "Critical effects of the polarity change in delayed states within an LTI dynamics with multiple delays," *IEEE Transactions on Automatic Control*, vol. 60, no. 11, pp. 3018–3022, 2015.

[28] Q. Gao and N. Olgac, "Bounds of imaginary spectra of LTI systems in the domain of two of the multiple time delays," *Automatica*, vol. 72, pp. 235–241, 2016.

[29] ——, "Stability analysis for LTI systems with multiple time delays using the bounds of its imaginary spectra," *Systems & Control Letters*, vol. 102, pp. 112–118, 2017.

[30] R. Cepeda-Gomez and N. Olgac, "An exact method for the stability analysis of linear consensus protocols with time delay," *IEEE Transactions on Automatic Control*, vol. 56, no. 7, pp. 1734–1740, 2011.

[31] Y. Cao and W. Ren, "Distributed coordinated tracking with reduced interaction via a variable structure approach," *IEEE Transactions on Automatic Control*, vol. 57, no. 1, pp. 33–48, 2012.

[32] T. Yucelen and J. D. Peterson, "Active-passive networked multiagent systems," in *IEEE Conference on Decision and Control*, 2014, pp. 6939–6944.

[33] D. Shevitz and B. Paden, "Lyapunov stability theory of nonsmooth systems," in *IEEE Conference on Decision and Control*, 1993, pp. 416–421.

[34] R. G. Bartle and D. R. Sherbert, *Introduction to real analysis*. Hoboken, NJ: Wiley, 2011.

[35] J. Li, W. Ren, and S. Xu, "Distributed containment control with multiple dynamic leaders for double-integrator dynamics using only position measurements," *IEEE Transactions on Automatic Control*, vol. 57, no. 6, pp. 1553–1559, 2012.

[36] M. M. Zavlanos, A. Jadbabaie, and G. J. Pappas, "Flocking while preserving network connectivity," in *IEEE Conference on Decision and Control*, 2007, pp. 2919–2924.

[37] M. M. Zavlanos and G. J. Pappas, "Distributed connectivity control of mobile networks," *IEEE Transactions on Robotics*, vol. 24, no. 6, pp. 1416–1428, 2008.

[38] K. B. Petersen and M. S. Pedersen, "The matrix cookbook," November 2012, version 20121115. [Online]. Available: http://www2.imm.dtu.dk/pubdb/p.php?3274

[39] H. Safadi, "Local path planning using virtual potential field," *McGill University School of Computer Science, Tech. Rep*, 2007.

[40] J.-O. Kim and P. K. Khosla, "Real-time obstacle avoidance using harmonic potential functions," *IEEE Transactions on Robotics and Automation*, vol. 8, no. 3, pp. 338–349, 1992.

[41] T. Balch, "Avoiding the past: a simple but effective strategy for reactive navigation," in *IEEE International Conference on Robotics and Automation*, 1993, pp. 678–685.